

# Influence of magnetic field on the paramagnetic-ferromagnetic transition in a $\text{La}_{1-x}\text{Ca}_x\text{MnO}_3$ ( $x \approx 0.25$ ) crystal: Ultrasonic and transport studies

B. I. Belevtsev,<sup>1,\*</sup> G. A. Zvyagina,<sup>1</sup> K. R. Zhekov,<sup>1</sup> I. G. Kolobov,<sup>1</sup> E. Yu. Beliayev,<sup>1</sup> A. S. Panfilov,<sup>1</sup> N. N. Galtsov,<sup>1</sup> A. I. Prokhvatilov,<sup>1</sup> and J. Fink-Finowicki<sup>2</sup>

<sup>1</sup>*B. Verkin Institute for Low Temperature Physics and Engineering, National Academy of Sciences, pr. Lenina 47, Kharkov 61103, Ukraine*

<sup>2</sup>*Institute of Physics, Polish Academy of Sciences, 32/46 Al. Lotnikow, 02-668 Warsaw, Poland*

(Received 5 April 2006; revised manuscript received 29 June 2006; published 23 August 2006)

The ultrasonic properties of  $\text{La}_{1-x}\text{Ca}_x\text{MnO}_3$  ( $x \approx 0.25$ ) with the Curie temperature  $T_C$  about 200 K are studied. Temperature dependences of longitudinal and transverse sound velocities were measured in zero magnetic field and for different constant magnetic fields as well. The ultrasonic study is supported by magnetic, resistive, magnetoresistive, structural, and other measurements of the sample that facilitate interpretation of the results obtained. The magnetic-field influence on sound properties found in this study presents some interesting features of the interplay between the elastic and magnetic properties of these compounds. It is shown that the paramagnetic-ferromagnetic transition in the sample studied is first order, but can become second order under the influence of applied magnetic field.

DOI: [10.1103/PhysRevB.74.054427](https://doi.org/10.1103/PhysRevB.74.054427)

PACS number(s): 75.47.Lx, 62.80.+f, 75.47.Gk, 75.30.Kz

## I. INTRODUCTION

The magnetic and magnetoresistive properties of mixed-valence manganites of the type  $R_{1-x}A_x\text{MnO}_3$  (where  $R$  is a rare-earth element or La,  $A$  is a divalent alkaline-earth element) attracted much attention of scientific community in the last decade (see reviews, Refs. 1–3). A huge negative magnetoresistance (MR) near the Curie temperature of the paramagnetic-ferromagnetic transition,  $T_C$ , was observed for lanthanum manganites ( $R=\text{La}$ ) with  $0.2 \leq x \leq 0.5$ . This phenomenon, called “colossal” magnetoresistance (CMR), is viewed as promising to advanced technology. This and other unique properties of mixed-valence manganites are determined by the complex spin, charge, and orbital ordered phases, and therefore are of a great fundamental interest for physics of strongly correlated electrons.

In spite of enormous theoretical and experimental activity in the area of CMR manganites many questions remain unresolved. For example, a lot of theoretical models are developed for CMR, but they are so diverse that it is difficult to choose between them. Moreover, a quantitative comparison of the known models with experiment is practically impossible (or too ambiguous). For this reason no definite consensus is reached yet about the essential nature of CMR.<sup>4</sup>

It is clear that a variety of experimental methods must be used to make progress in the physics of these complex compounds. Among these the ultrasonic investigations are very helpful ones, and were used therefore fairly often, since they can give an important information about manganites’ elastic properties and how these properties vary at magnetic transitions. Really, it is well known that any magnetic transition or even changes in magnetic properties with temperature or magnetic field are accompanied by transformation or, at least, some spontaneous deformation of crystal lattice.<sup>5</sup> For this reason the sound velocity and elastic properties are rather sensitive to changes in magnetic state. In this paper we present an ultrasonic investigation of a bulk manganite  $\text{La}_{1-x}\text{Ca}_x\text{MnO}_3$  ( $x \approx 0.25$ ) prepared by the floating-zone

method. The study has been done at various magnetic fields that makes the data obtained more informative. The known ultrasonic studies of  $\text{La}_{1-x}\text{Ca}_x\text{MnO}_3$  system were usually carried out in zero magnetic field, although some studies in magnetic fields for manganites of other types are known (and will be discussed below). Since any experimental method alone is not enough for proper study of such complex compounds, the ultrasonic study was supported by structural, magnetic, and transport measurements. All this has enabled us to arrive at some definite conclusions about peculiarities of magnetic states and paramagnetic-ferromagnetic (PM-FM) transition in this type of manganites. In particular, we have shown that the PM-FM transition is first order, but can become second order under the influence of applied magnetic field.

## II. EXPERIMENT

The crystal under study was grown (at the Institute of Physics, Warsaw) by the floating-zone method using a ceramic feed rod with a nominal composition  $\text{La}_{0.67}\text{Ca}_{0.33}\text{MnO}_3$ . The crystal growing procedure is outlined in Ref. 6 where it was shown that crystal perfection of samples produced by the described technique is close to that of single crystals, and, in this respect, they have far better crystal quality and far less porosity than the samples prepared by a solid-state reaction technique. On the other hand, the crystals have some extrinsic inhomogeneities arising due to technological factors in the sample preparation. These are rare grain boundaries and twins.<sup>6</sup>

The sample characterization and measurements were done by a variety of experimental techniques. The structure state of the sample was studied by the x-ray diffraction (XRD) method. The XRD spectra (from prepared powders) were obtained using a DRON-3M diffractometer with the  $K_\alpha$  radiation of the Cu anode. The errors in the intensity of diffraction peaks and the deduced lattice parameters were 1% and 0.02%, respectively. The x-ray study in a Laue camera

has been done as well. The dc magnetization was measured in a homemade Faraday-type magnetometer. Resistance as a function of magnetic field (up to 1.7 T) and temperature (in the range 4–400 K) was measured using a standard four-point probe technique in a homemade cryostat.

Acoustic properties (sound wave velocity and attenuation) were measured with a new version of the phase method described in Ref. 7. The use of the electron-controllable phase shifter together with the digital phasemeter permitted us to gain the resolution about one degree at practically unlimited dynamic range. The method permits us to measure the absolute values of the sound velocities in samples on the one hand, and to register the relative changes in the sound velocities and attenuation as a function of temperature or magnetic field, on the other hand. The method can give an acceptable accuracy ( $\approx 1\%$ ) for the absolute value of the sound velocity in samples of a millimeter (submillimeter) size. The standard accuracies of the measurements for the relative changes of the sound velocity and the sound attenuation were  $10^{-4}$  and 0.05 dB, respectively.

The measurements (in zero magnetic field and for different magnitudes of the field up to 4 T) were carried out with longitudinal and transversal waves (in the frequency range 53–55 MHz) applied to the sample studied. The magnetic field has always been applied in the direction of the propagation vector of sound waves.

We used the sample with the dimensions  $2.94 \times 1.9 \times 1.8$  mm<sup>3</sup> in our acoustic investigation. The working surfaces of the sample were carefully processed using fine abrasive powder and were made flatly parallel (with the accuracy 1–2  $\mu$ m). To obtain the acoustic contact between piezoelectric transducers and working surfaces of the samples we used bonding layers of the oil GKZh-94 and the glue BF-2 for the measurements of the longitudinal and transversal waves, respectively. The GKZh-94 is an organic silicone polymer oil. It stays in a liquid phase until 120 K, and hence an additional stress on the sample in the region of the phase transition (200 K) is excluded. The glue BF-2 (alcohol solution of Bakelite and polyvinylbutyral) is polymerized at the room temperature. Since the features in the temperature behavior of the transversal sound appear at the same temperatures, as for the longitudinal one, we can conclude that the bonding layers do not significantly affect the results of the measurements.

### III. RESULTS AND DISCUSSION

#### A. General characterization of the sample

The disc-shaped samples cut from the same cylindrical crystal (about 8 mm in diameter) were used for different kinds of investigations. The resistive and magnetoresistive properties for one of such discs are described in Ref. 6. It was shown in that study, among other things, that the inner part of the disc appeared to be more homogeneous and perfect than the outer part. For this reason only the central part (with the diameter about 4.5 mm) of the disc chosen for this study has been used for ultrasonic and all other measurements described in this paper. It turned out that the sample studied had somewhat different magnetic and transport prop-

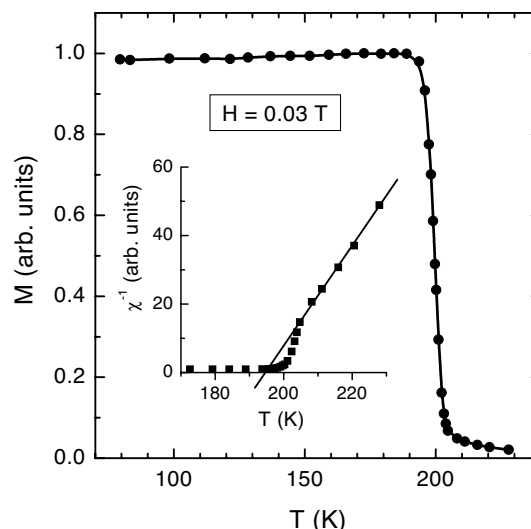


FIG. 1. Temperature dependence of magnetization for the  $\text{La}_{0.75}\text{Ca}_{0.25}\text{MnO}_3$  crystal (recorded in a dc magnetic field  $H = 0.03$  T with increasing temperature after the sample was cooled in zero field). The inset shows the temperature behavior of the inverse susceptibility  $1/\chi$  in the paramagnetic region at the same field.

erties as compared with the sample described in Ref. 6, although both samples were cut from the same grown cylindrical crystal. For example, the Curie temperature  $T_C$  which was taken as the temperature of the inflection point in the temperature dependence of magnetization was equal to about 200 K in the sample studied (Fig. 1) compared with  $T_C \approx 216$  K found in Ref. 6. The temperature dependences of resistance  $R(T)$  and magnetoresistance (MR) are also found to be somewhat different from that in Ref. 6 (see below).

The reason for distinctions in magnetic and other properties of the samples taken from different parts of the same grown crystal can be considered as rather clear. It is known<sup>8</sup> that  $\text{La}_{1-x}\text{Ca}_x\text{MnO}_3$  crystals grown by floating-zone technique have an inhomogeneous distribution of La and Ca along the growth direction. The initial part of the crystal is usually somewhat enriched in La and depleted in Ca. The microprobe elemental analysis of the sample in Ref. 6 had shown that its chemical composition was close to the nominal one ( $x=0.33$ ). In contrast to this, the electron microprobe analysis in a scanning electron microscope ISM-820 has shown that for the sample studied in this work the elemental ratio  $\text{Ca}/(\text{La}+\text{Ca})$  is about 0.25. The ratio  $(\text{La}+\text{Ca})/\text{Mn}$  has been found to be somewhat larger than unity (about 1.1), that can be an evidence of some Mn deficiency.

The sample was characterized also by XRD from powder. It is known that bulk  $\text{La}_{1-x}\text{Ca}_x\text{MnO}_3$  has a distorted perovskite structure, which presently is believed to be orthorhombic.<sup>2,3</sup> In the orthorhombic space group  $Pnma$ , lattice constants are  $a \approx \sqrt{2}a_p$ ,  $b \approx 2a_p$ , and  $c \approx \sqrt{2}a_p$ , where  $a_p$  is the lattice constant of pseudocubic perovskite lattice. Generally, however, the deviations from cubic symmetry are found to be fairly small, especially in the CMR range ( $0.2 < x < 0.5$ ).<sup>9,10</sup> It is found in this study that the powder XRD spectra of the sample at  $T=293$  K is consistent with the orthorhombic  $Pnma$  lattice with lattice constants  $a$

$a=0.54855$  nm,  $b=0.77652$  nm, and  $c=0.54994$  nm. It is seen that the orthorhombic distortions are rather small that permits us to determine from these data the average cubic lattice constant  $a_p=0.38834$  nm. This is a little larger than that ( $a_p=0.38713$  nm) obtained in Ref. 6 for the sample with the composition close to the nominal one ( $x=0.33$ ). But this is quite expected since  $a_p$  becomes larger with decreasing Ca content  $x$  in  $\text{La}_{1-x}\text{Ca}_x\text{MnO}_3$  manganites.<sup>9</sup>

The crystal perfection of the sample studied has also been proved by x-ray study with a Laue camera. This revealed that the XRD pattern of a small piece taken from the central part of the sample corresponds to a single-crystal structure. The sample as a whole is not, however, a single crystal but consists of a few grains.

It is known that the  $T_C$  value in  $\text{La}_{1-x}\text{Ca}_x\text{MnO}_3$  system decreases rather sharply with decreasing  $x$  in the range  $0.2 \leq x \leq 0.3$ .<sup>1-3,11</sup> In crystals prepared by the floating-zone method the  $T_C$  values equal to 216, 200, and 189 K were found for  $x=0.3$ ,<sup>12</sup> 0.25,<sup>10</sup> and 0.22,<sup>13</sup> respectively.<sup>14</sup> Thus the value of  $T_C \approx 200$  K in the sample studied is equal to that expected for  $x=0.25$  in  $\text{La}_{1-x}\text{Ca}_x\text{MnO}_3$  crystals prepared by floating-zone method. The same value of  $T_C$  also follows from the resistive and magnetoresistive properties of the sample (described in the next section) which in addition to that give evidence of rather high crystal perfection of the sample.

The magnetization data (Fig. 1) allow us to make some general suggestions about the nature of the PM-FM transition in the sample studied. It can be seen that the magnetic transition is notably sharp and the  $M(T)$  behavior obviously does not follow the classical molecular-field theory for the PM-FM transition.<sup>5</sup> The transition does not appear as a second-order one, but more likely as a slightly broadened first-order transition. The inset in Fig. 1 shows the temperature behavior of the inverse susceptibility ( $1/\chi=H/M$ ) above  $T_C$ . It is seen that  $1/\chi(T)$  does not follow the Curie-Weiss law in the paramagnetic region and has a characteristic knee. This particular kind of deviations from the Curie-Weiss law [with  $T_{pm} < T_C$ , where  $T_{pm}$  is determined by extrapolation of the linear part of the  $1/\chi(T)$  curve down to the intersection with the  $T$  axis;  $T_C$  is the Curie temperature defined from the  $M(T)$  curve] had previously been found in  $\text{La}_{1-x}\text{Ca}_x\text{MnO}_3$  manganites with  $x \approx 0.25$  or close to this,<sup>15-17</sup> and had been interpreted as a feature of first-order transition.<sup>16</sup> Generally, however, the nature of the ferromagnetic transition in La-Ca manganites in the region  $0.2 \leq x \leq 0.3$  is still not so clear and may be influenced by intrinsic and extrinsic inhomogeneities.<sup>4,11,17</sup> For example, the above-mentioned knee-type feature in the  $1/\chi(T)$  dependence above  $T_C$  (like that in the inset of Fig. 1) has been attributed in Ref. 17 to the appearance of spin-aligned (ferromagnetic) clusters above  $T_C$ . The cluster size grows as the temperature becomes closer to  $T_C$  (or with increasing magnetic field) so that the magnetic transition is governed by percolation processes (see discussion in Ref. 4).

### B. Resistive and magnetoresistive properties

The temperature dependences of resistivity  $\rho$  and MR are shown in Figs. 2–4. The  $\rho(T)$  curve in Fig. 2 for zero mag-

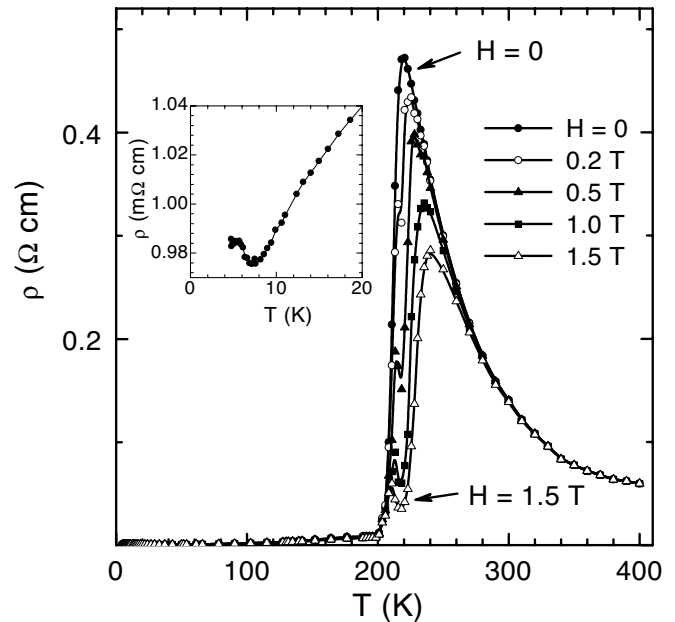


FIG. 2. Temperature dependences of the resistivity for the  $\text{La}_{0.75}\text{Ca}_{0.25}\text{MnO}_3$  crystal, recorded in zero magnetic field and in fields  $H=0.2, 0.5, 1,$  and  $1.5$  T. The inset shows a shallow resistance minimum at temperature  $T_{min} \approx 7.4$  K.

netic field shows an impressively huge (50-fold) drop of the resistivity when crossing  $T_C$  from above. Note that after this drop the resistance continues to decrease changing further nearly by the order of magnitude with decreasing temperature (Fig. 3). In La-Ca manganites,  $\rho(T)$  has a semiconducting behavior above  $T_C$  and metallic behavior below  $T_C$  which results in a resistivity peak at  $T=T_p$  (Figs. 2 and 3). For the sample studied, resistivity above  $T_C$  (in the paramagnetic state) follows  $\rho(T) \propto \exp(E_a/T)$  with  $E_a=0.1$  eV. This is in

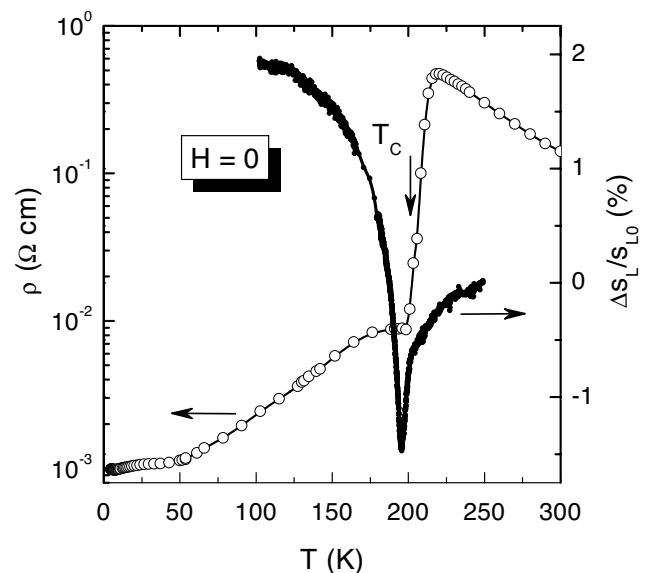


FIG. 3. Comparison of temperature variations of the resistivity and the longitudinal sound velocity (taken on heating) in the crystal studied in zero field. The position of  $T_c$  is shown by an arrow.

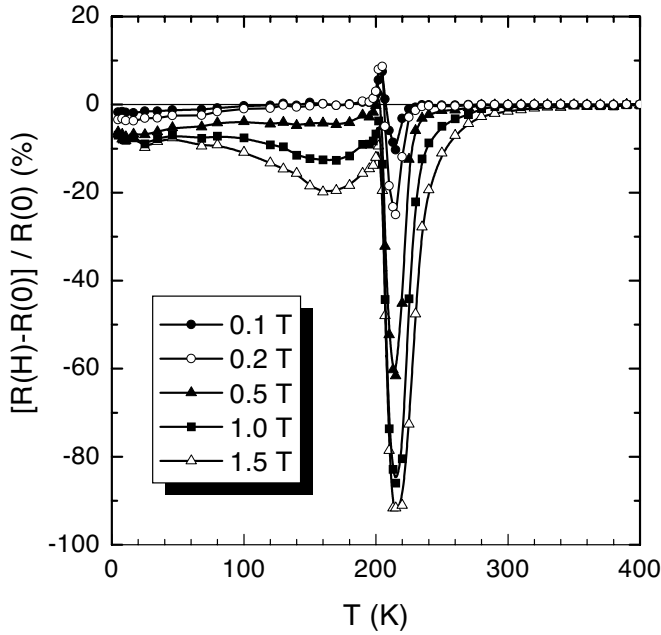


FIG. 4. Temperature dependences of magnetoresistance for the sample studied, recorded at different magnitudes of applied magnetic field.

good agreement with that (about 0.1 eV) reported by other authors for  $\text{La}_{1-x}\text{Ca}_x\text{MnO}_3$  crystals with nearly the same composition.<sup>2,6,12</sup> In the low-temperature range,  $\rho(T)$  has a minimum at  $T_{\min} \approx 7.4$  K (Fig. 2).

The sample possesses huge MR (Figs. 2 and 4). Taking a quantity  $\Delta R(H)/R(0) = [R(H) - R(0)]/R(0)$  as a measure of MR, the maximum absolute values of  $\Delta R(H)/R(0)$  equal to 86% and 91.7% can be determined near  $T \approx T_C$  for fields 1 and 1.5 T, respectively. This really colossal MR (in not that strong fields (note that  $|\Delta R(H)|/R(0)$  by definition cannot be higher than 100%) is an evidence of high crystal perfection of the sample studied. Another important measure of crystal perfection in manganites is the ratio,  $\rho(T_p)/\rho(0)$ , of peak resistivity  $\rho(T_p)$  and the residual resistivity at low temperature ( $T \approx 4$  K),  $\rho(0)$ . The value of  $\rho(T_p)/\rho(0)$  is about 480 for the sample studied with  $\rho(0) \approx 10^{-3} \Omega \text{ cm}$ .

On the whole, resistive and magnetoresistive behavior of the sample studied (with  $x \approx 0.25$ ) is fairly close to that of the sample taken from another part of the grown crystal with  $x \approx 0.33$  (described in Ref. 6). This includes specific features of the  $\rho(T)$  and  $\Delta R(H)/R(0)$  dependences, such as shouldered form of  $\rho(T)$  and the low-temperature resistance minimum (Figs. 2 and 3), and double-peaked appearance of the temperature dependences of MR for high enough fields (Fig. 4). These features were fully considered and elucidated in Ref. 6, and will not be retold in this paper.<sup>18</sup> It should only be mentioned that the sharp peaks in  $\rho(T)$  and MR near  $T_C$  (Figs. 2 and 4) are determined by the transition from the insulating paramagnetic to metallic ferromagnetic phase in a considerable part of the sample volume; whereas the shoulder in  $\rho(T)$  (Fig. 3) and the second weak peak in the temperature dependence of MR (Fig. 4) are determined by the presence of grain-boundary-like inhomogeneities which in

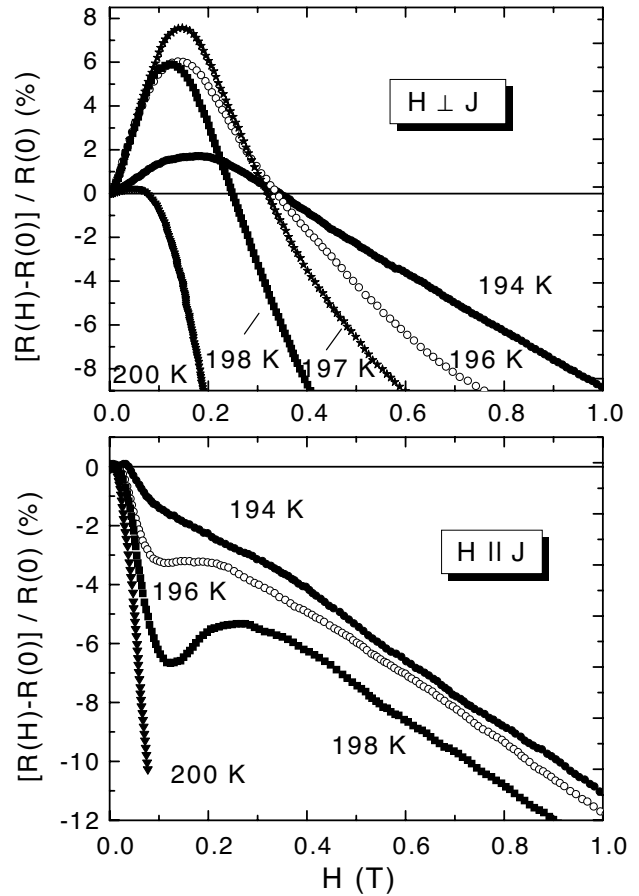


FIG. 5. Magnetoresistance of the sample studied for different temperatures near  $T_C \approx 200$  K for parallel and perpendicular orientations of the magnetic field relative to the measuring current  $J$ .

the crystals grown by the floating-zone method are most likely twin boundaries.<sup>6,19</sup>

Figure 4 shows a pronounced positive MR which appears only for low-field range and peaks near  $T_C$ . It should be noted that the temperature dependences of the MR in Fig. 4 were recorded for magnetic-field orientation perpendicular to the measuring current  $J$ . When applied field is parallel to the current, the MR is always negative [compare  $\Delta R(H)/R(0)$  dependences near  $T_C$  for  $H \parallel J$  and  $H \perp J$  in Fig. 5]. Thus a considerable MR anisotropy is found in the sample studied near  $T_C$ . This effect has not been seen in the study<sup>6</sup> of other pieces of the same grown crystal because the low-field MR was not investigated there.

The MR anisotropy effect found is very interesting by itself, but is not the main goal of the present study and will be touched here only in general. In bulk ferromagnetic samples, the dependence of resistance on the angle between electric current and magnetic field should actually reflect a corresponding dependence of resistance on the angle between current and magnetization. The MR anisotropy in the sample studied should be primarily associated with the so-called anisotropic MR (AMR) effect, determined by spin-orbit coupling.<sup>20</sup> AMR is the intrinsic property of ferromagnets and depends on the relative orientation of the magnetization and current. The effect is well known for

CMR manganite films (see Refs. 21–23 and references therein), but has not been mentioned previously in known literature for bulk manganite samples.

The following quantity can be used as a measure of the AMR:

$$\delta_{an}(T, H) = \frac{R_{\parallel}(T, H) - R_{\perp}(T, H)}{R_0(T)},$$

where  $R_{\parallel}$  and  $R_{\perp}$  are longitudinal ( $M \parallel J$ ) and transverse ( $M \perp J$ ) resistances, respectively;  $R_0(T)$  is zero field resistance. The applied magnetic field must be high enough to rotate the magnetization in a selected direction. It was found<sup>21–23</sup> that  $\delta_{an}$  is negative for manganite films (in contrast to 3d metals and alloys where it is usually positive) and is a maximum at  $T \approx T_C$ . In this regard, the MR anisotropy found in this study for the bulk manganite crystal behaves like that for manganite films. There is, however, a significant difference in the magnitude of the effect. The maximum absolute value of  $\delta_{an}$  near  $T_C$  for the films is 1–2%.<sup>21–23</sup> This rather small magnitude (in comparison with that known for 3d metals<sup>20</sup>) was even justified for manganites in the frame of the approach developed for 3d metals.<sup>22</sup> In the sample studied, the maximum magnitude of  $\delta_{an}$  (about 15%, as can be estimated from Fig. 5) is, however, far higher. It should be noted that in ferromagnetic films, besides the AMR effect, some further sources of MR anisotropy are inevitably present,<sup>21</sup> for example, the existence of preferential directions of magnetization due to strains stemming from the lattice film-substrate mismatch, the influence of the shape anisotropy, and other sources. In bulk samples these factors are either absent or not so important. Magnetocrystalline anisotropy in manganites with nearly cubic-lattice symmetry<sup>9,10</sup> is negligible and therefore cannot exert much influence on MR anisotropy in bulk samples. It is known as well that the AMR effect in manganite films becomes apparent only in samples with fairly high crystal perfection.<sup>23</sup> Maybe for some of these reasons  $\delta_{an}$  is so high in the rather perfect bulk crystal studied. It can be said, to summarize, that the problem of the AMR in manganites cannot be considered as quite clear and further theoretical and experimental work in this direction is needed.

### C. Ultrasonic properties near the PM-FM transition

Before presenting ultrasonic results obtained, we will mention briefly the known ultrasonic studies of the PM-FM transition in the  $\text{La}_{1-x}\text{Ca}_x\text{MnO}_3$  system. It was generally revealed (on ceramic samples with chemical composition similar to that of the sample studied; see, for example, Refs. 1,24,25) that both the longitudinal and transverse sound velocities begin to increase continuously when crossing  $T_C$  from above, amounting to values up to  $\approx 5\%$  larger than those above  $T_C$ . The sound attenuation shows a rather sharp peak at  $T \approx T_C$ . An external magnetic field suppresses this sound anomaly in the neighborhood of  $T_C$ .<sup>1,24</sup> In other studies<sup>26,27</sup> of La-Ca manganites (made as we believe on samples with higher crystal perfection) the temperature dependence of sound velocity was found to reveal a weak but quite clear minimum near  $T_C$ , that is, with decreasing temperature the

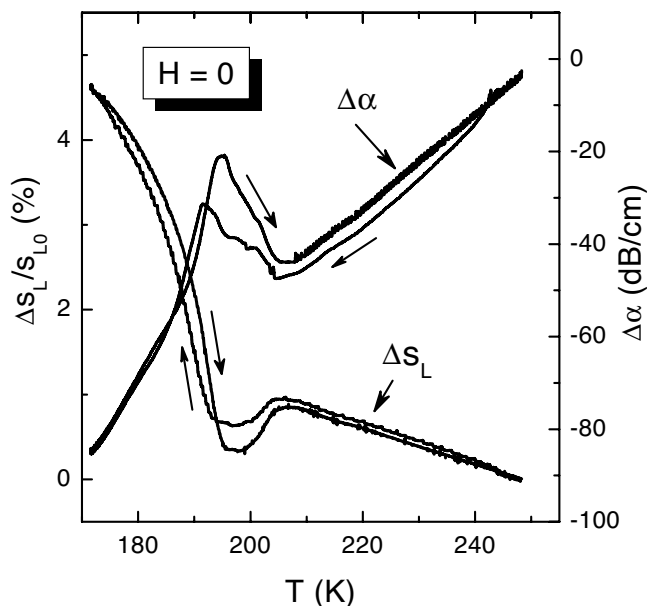


FIG. 6. Relative changes in the longitudinal sound velocity  $s_L$  and sound attenuation  $\alpha$  in the region around Curie temperature  $T_C \approx 200$  K at zero magnetic field. The arrows near the curves show directions of temperature variations during measurements (heating and cooling). Both heating and cooling rates were about 0.16 K/min.

sound velocity first decreases noticeably when approaching  $T_C$  (so-called softening) and then increases after crossing  $T_C$ . The same behavior was found in La-Sr manganite ( $\text{La}_{0.67}\text{Sr}_{0.33}\text{MnO}_3$ ) near the PM-FM transition.<sup>28</sup>

The sample studied, although being rather perfect, consists, however, of large crystals with different orientations, so that our ultrasonic study is carried out as that for a polycrystalline sample. Temperature dependences of the longitudinal sound velocity  $s_L$  and attenuation  $\alpha$  measured in this work (Figs. 3 and 6) show clear anomalies in the region near  $T_C \approx 200$  K: a minimum in  $s_L(T)$  and a peak in the attenuation, that agrees with data of Refs. 26 and 27. The minimum in  $s_L(T)$  appears to be, however, much more expressive and sharper as compared with that in Refs. 26 and 27. In this respect, this anomaly is more similar to a considerable sound velocity softening found in the vicinity of the charge-ordering transition temperature  $T_{CO}$  in  $\text{La}_{1-x}\text{Ca}_x\text{MnO}_3$  for Ca concentrations around  $x \approx 0.2$  and  $0.5 \leq x \leq 0.82$ .<sup>1,24,25,29</sup> According to Ref. 29, it should be attributed to large local volume fluctuations which are caused by the two-phase competition near the transition temperature. The same reason can be responsible for the sharp minimum in  $s_L(T)$  near  $T_C$  under the PM-FM transition in the sample studied.

The  $s_L(T)$  and  $\alpha(T)$  dependences are hysteretic in a rather wide region around the PM-FM transition. This clearly indicates that the transition is more in the nature of the first-order one, that also follows from the temperature behavior of the inverse susceptibility  $1/\chi$  in the paramagnetic region (inset in Fig. 1). The temperature dependence of the transverse sound velocity  $s_T$  (Fig. 7) shows an increased slope in the region of  $T_C$  with a considerable change in the slope below  $T_C$ , but generally the  $s_T(T)$  curve does not demonstrate some clear features around  $T_C$ .

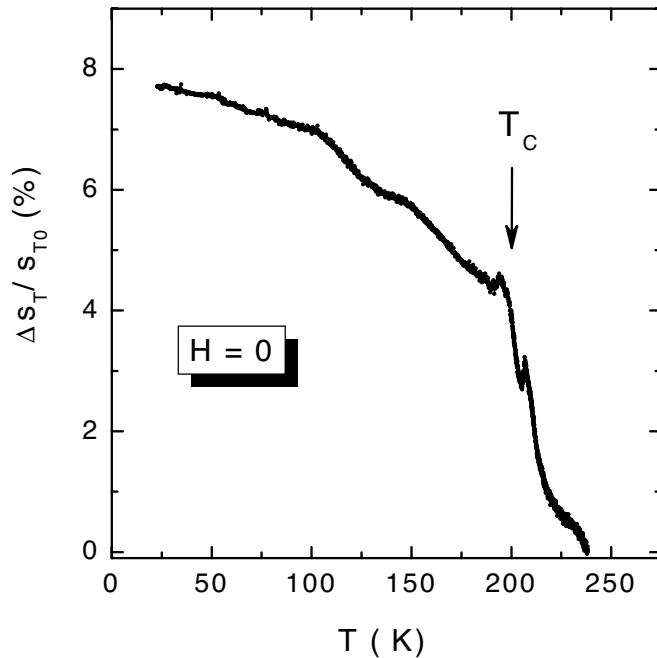


FIG. 7. Relative changes in the transverse sound velocity  $s_T$  in the region around Curie temperature  $T_C \approx 200$  K at zero magnetic field. The dependence was taken on heating with rate about 0.16 K/min.

Figures 6 and 7 show the relative temperature variations of the longitudinal  $s_L$  and transverse  $s_T$  sound velocities. The absolute values of the sound velocities have been measured at  $T=77$  K. The following values were obtained:  $s_L=6.4 \times 10^5$  cm/s and  $s_T=2.65 \times 10^5$  cm/s for the sample with acoustical path 2.94 mm. They agree fairly well with those obtained by other researchers in La-Ca manganites of the approximate chemical composition.<sup>29,30</sup> Figure 3 demonstrates a comparison of temperature variations of the longitudinal sound velocity and the resistivity (both taken on heating) in the crystal studied. It is seen that the temperature position of the sound anomaly agrees closely with the sharp drop in the resistance near  $T \approx T_C$ .

The influence of magnetic field on the  $s_L(T)$  anomaly in the region of the PM-FM transition is shown in Fig. 8. It is seen that the magnetic field up to 4 T does not suppress the sound-velocity anomaly significantly, as opposed to the data of Refs. 1 and 24. As a matter of fact, in our study the magnitude of the anomaly increases considerably and its width becomes broader with increasing applied field up to 2 T, and only in the highest applied field ( $H=4$  T) it reduces to some degree being still larger than that at zero field. The second important feature is that the temperature position of the anomaly [as a measure of which the temperature  $T_{tr}$  of the minimum in  $s_L(T)$  can be taken] moves steadily to higher temperature with increase in an external field. This is shown more clearly in Fig. 9 where magnetic-field dependence of the transition temperature  $T_{tr}$  is presented. Due to the considerable hysteresis (Fig. 6), the values of  $T_{tr}(H)$  taken from the  $s_L(T)$  curves on heating and cooling are considerably different. This difference reduces, however, nearly to zero with increasing magnetic field up to  $H=4$  T (Fig. 9). The attenu-

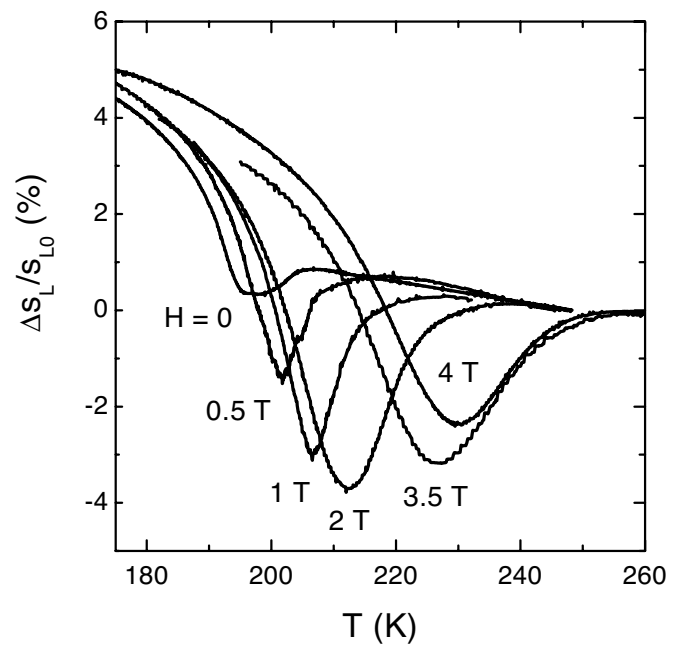


FIG. 8. Relative changes in longitudinal sound velocity  $s_L$  in temperature range near the paramagnetic-ferromagnetic transition in different magnetic fields. All curves (except at  $H=3.5$  T) were taken on heating.

ation peak for the longitudinal sound behaves in magnetic field in the same way as the sound-velocity anomaly: its position shifted steadily to higher temperature with increasing field, and the peak's magnitude depends on the field in the same nonmonotonic way.

The magnetic-field dependences of the longitudinal and transverse sound velocities are presented in Figs. 10 and 11. For longitudinal waves the magnetic-field behavior of the

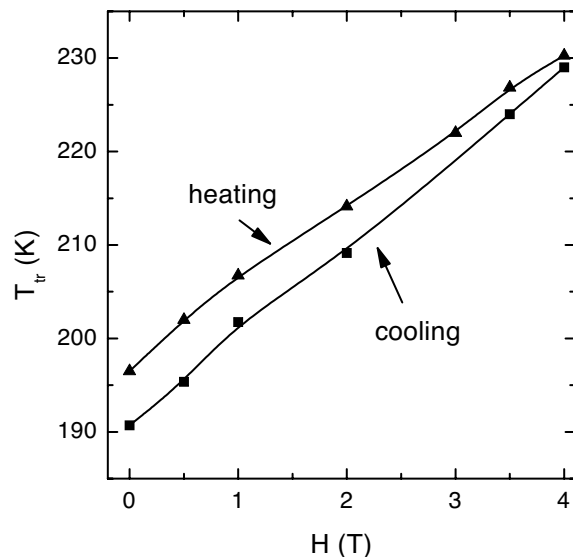


FIG. 9. Influence of magnetic field on the transition temperature  $T_{tr}$ . The temperature  $T_{tr}$  is defined as a position of the temperature minimum in  $s_L(T)$  curves (Fig. 8) in the region of the PM-FM transition. The values of  $T_{tr}(H)$  were taken from  $s_L(T)$  curves measured in different magnetic fields on heating and cooling.

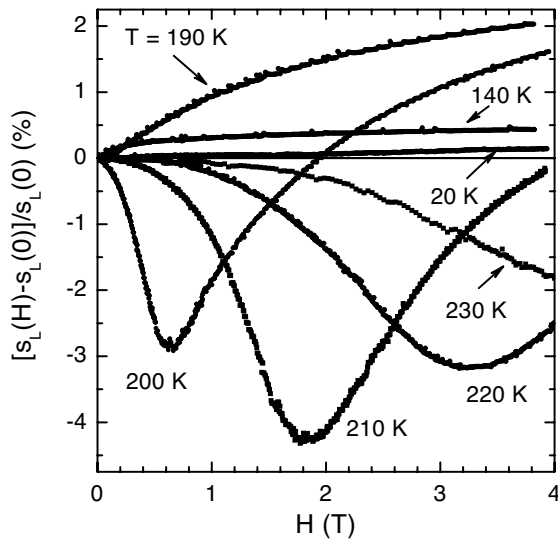


FIG. 10. Relative dependences of the longitudinal sound velocity on applied magnetic field recorded for different constant temperatures.

relative quantity  $[s_L(H) - s_L(0)]/s_L(0)$  [with  $s_L(0)$  being the sound velocity in zero field] is presented in Fig. 10. The similar quantity,  $[s_T(H) - s_T(0)]/s_T(0)$ , is used for the transverse velocity in Fig. 11, where the curves are somewhat shifted relative to each other to show more clearly the behavior of this parameter for different temperatures. These parameters present well-defined magnetosonic effect (MSE), which characterizes the influence of magnetic field on the longitudinal and transversal waves (much as, for example, the magnetoresistive effect is a similar characteristic for the resistivity). The longitudinal MSE is positive below  $T_C$  where it has a monotonic dependence on magnetic field (Fig. 10). It is very small for  $T \ll T_C$ , but increases with increasing temperature when going to  $T_C$ . But the behavior of the longitudinal MSE changes dramatically when temperature crosses  $T_C$  (Fig. 10). It becomes negative for  $T \geq T_C$  and its behavior in magnetic field becomes nonmonotonic. The field position of the minimum in MSE in this temperature range increases with increasing temperature. Actually, the  $(T, H)$  coordinates of these minima correspond rather closely to the phase diagram  $T_r$ - $H$  shown in Fig. 9. This indicates that the shift of the temperature  $T_r$  in magnetic field and shift of the magnetic-field position of the minimum in the MSE with increase in temperature are determined by processes of the same origin. These are related to magnetoelastic (or magnetostructural) interaction in the sample studied and will be discussed below. The transverse MSE (Fig. 11) behaves quite differently than the longitudinal one. It has a nonmonotonic (with minimum) magnetic-field behavior below  $T_C$  and the monotonic one above it. In the same manner as the longitudinal effect, the transverse MSE is negligible at low temperature  $T \ll T_C$ , but increases considerably with increasing temperature when moving to  $T_C$ .

The presently attained knowledge of the CMR manganites is quite enough for (at least) qualitative interpretation of the results obtained. The available literature indicates that significant changes in the crystal lattice and elastic properties of

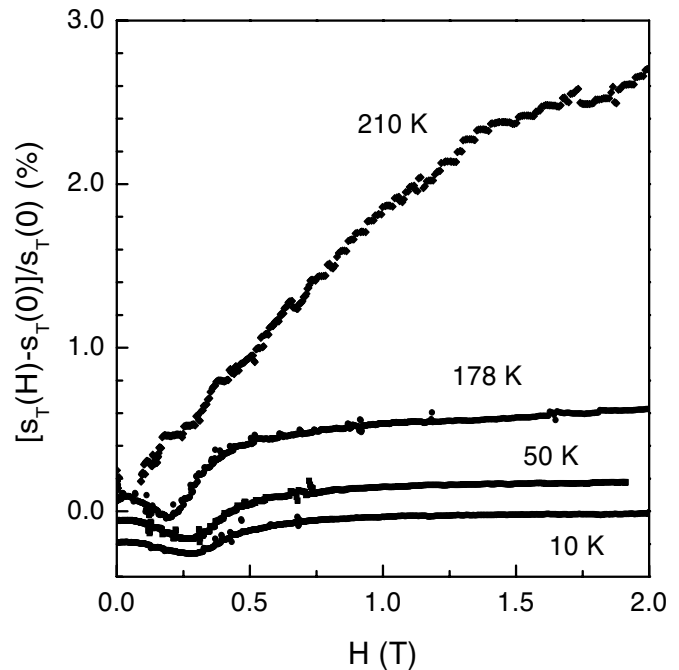


FIG. 11. Relative dependences of the transverse sound velocity on applied magnetic field recorded for different constant temperatures.

La-Ca manganites take place under the PM-FM transition or with strengthening of the FM order by an external influence. For example, the PM-FM transition in ceramic samples of  $\text{La}_{1-x}\text{Ca}_x\text{MnO}_3$  ( $0.25 \leq x \leq 0.35$ ) is known to be accompanied by a rather significant contraction of the crystal lattice, which causes a peak in the thermal-expansion coefficient near  $T_C$ .<sup>31-35</sup> Above  $T_C$ , the lattice expansion is enhanced compared with the prediction of the Grüneisen law. The large changes in the lattice unit-cell volume at the PM-FM transition is a doubtless evidence that this is a magnetostructural transition of first order. It is found for a La-Ca manganite sample with  $x=0.33$  (Ref. 34) that the increase in magnetic field in the temperature range near  $T_C$  (including  $T$  somewhat below or above it) causes a decrease in the unit-cell volume together with simultaneous increase in the saturated magnetization (in the region of the so-called paraprocess<sup>5</sup>). This shows clearly that strengthening of magnetic order in manganites results in contraction of the crystal lattice (and vice versa, as the studies of the pressure effect on  $T_C$  show<sup>2</sup>).

The magnetostriction study of Ref. 33 for La-Ca manganite with  $x=0.33$  appears to be helpful for understanding of ultrasonic data of this study. The authors of that study have measured longitudinal  $(\Delta l/l)_\parallel$ , transverse  $(\Delta l/l)_\perp$ , and volume  $\Delta V/V = (\Delta l/l)_\parallel + 2(\Delta l/l)_\perp$  magnetostrictions (MSs), and found that  $\Delta V/V$  is negative in a wide range around  $T_C$  with a maximum of its absolute value peaked at  $T \approx T_C$ . But for  $T \leq T_C/2$  it becomes positive. The MS is isotropic  $[(\Delta l/l)_\parallel \approx (\Delta l/l)_\perp]$  in a rather wide range above  $T_C$  and in some narrower range below it. When moving further below  $T_C$ , the temperature behaviors of the longitudinal and transverse MS become, however, quite different:  $(\Delta l/l)_\parallel$  changes sign and becomes positive of an appreciable value with decreasing

temperature; whereas  $(\Delta l/l)_\perp$ , being negative, approaches nearly zero value with decreasing temperature, and only at low temperature (below 50 K) it attains a rather small positive value.

Besides the appreciable lattice volume changes, noticeable changes in local lattice structure take place as a result of the PM-FM transition or with strengthening of the FM order under the influence of magnetic field.<sup>10,32,34–38</sup> Bulk  $\text{La}_{1-x}\text{Ca}_x\text{MnO}_3$  has a distorted perovskite structure, which (to a fairly good approximation) is orthorhombic. The orthorhombic deformation of the cubic perovskite lattice is determined by the so-called  $\text{GdFeO}_3$  rotation of  $\text{MnO}_6$  octahedra and the Jahn-Teller (JT) distortion.<sup>3,10</sup> For the concentration range  $0.25 \leq x \leq 0.5$ , the JT distortion is found to be rather small,<sup>10,35</sup> but cannot be entirely neglected. In mixed-valence manganites, containing JT  $\text{Mn}^{3+}$  ions, the local JT distortions of  $\text{MnO}_6$  octahedra should be taken into account, even if the average JT distortion is negligible. The existing data on this matter are still rather incomplete and discrepant, but they allow us, nevertheless, to suppose that transition from the PM to FM state results in decrease in the orthorhombic and JT distortions. For example, in the La-Ca manganites with  $0.25 \leq x \leq 0.33$  the JT distortion decreases considerably when the system is going from the PM to the FM state.<sup>35–37</sup> The Mn-O-Mn bond angle increases;<sup>36</sup> whereas  $\text{GdFeO}_3$  rotation of  $\text{MnO}_6$  octahedra decreases<sup>10</sup> in the FM state, that testifies to a lessening of the orthorhombic distortions in this state. Since undistorted  $\text{MnO}_6$  octahedra are ascribed to the metallic FM phase, whereas the JT distorted octahedra are attributed to the PM insulating phase, it is reasonably suggested that in the transition region on both sides of  $T_C$  the charge localized and delocalized phases coexist.<sup>37</sup> The strengthening of the magnetic order above  $T_C$  induced by external field about 2 T causes a decrease in the orthorhombic and JT distortions in  $\text{La}_{0.75}\text{Ca}_{0.25}\text{MnO}_3$ .<sup>38</sup> It can be concluded therefore that enhancing of the magnetic order for any reason leads to relief of the orthorhombic and JT distortions.

It is known that fluctuations of the magnetic order and lattice volume near magnetic transitions cause increased absorption and hindered propagation of the sound at the Curie and Néel temperatures. For this reason, in many magnetic materials a sharp peak in the ultrasonic attenuation together with a sharp dip in the longitudinal sound velocity are frequently observed near the temperature of magnetic transitions.<sup>39–41</sup> For the transitions, which can be considered as second order, the inhomogeneous magnetic state near the critical point  $T_C$  is thought to be determined by the thermodynamic fluctuations of the spin order.<sup>5</sup> The PM-FM transition in the sample studied is undoubtedly first order. An inhomogeneous magnetic state near  $T_C$  is inherent for this type of phase transition as well. In La-Ca manganites with  $0.25 \leq x \leq 0.5$ , the multiphase coexistence near  $T_C$  can be determined by various reasons.<sup>2,4,37,42</sup> Beside the PM and FM phases, this multiphase state can include even nanoclusters of the antiferromagnetic phase.<sup>43</sup> It is found, in particular, that FM clusters are present well above  $T_C$  while some PM insulating clusters can persist down to a range far below  $T_C$ . This implies that the PM-FM transition has a percolative character. With decreasing temperature, the PM volume fraction decreases and that of the FM fraction increases. Since

the PM phase is insulating and the FM one is metallic, some kind of insulator-metal transition takes place near  $T_C$ . Beside this the PM phase has an increased lattice unit-cell volume. All these factors cause anomalies in ultrasonic properties near  $T_C$ .

The ultrasonic anomalies near  $T_C$  in the  $\text{La}_{0.75}\text{Ca}_{0.25}\text{MnO}_3$  manganite found in this study are determined by magnetoelastic (spin-phonon) interaction. The existent theories of these anomalies are developed primarily for second-order transitions,<sup>39–41</sup> but their main ideas can be used for first-order transitions as well. Besides, the latent heat for the PM-FM transition in La-Ca manganites of the approximate composition is rather small<sup>44,45</sup> so that this transition is not so far from second-order one. According to the models,<sup>39–41</sup> the spin-phonon interaction responsible for the ultrasonic anomalies in most cases comes from the strain modulation of the exchange interaction (volume magnetostrictive coupling). Although these models take into account the linear MS as well, we will consider in good approximation only the influence of the volume MS which dominates over the linear one for any ferromagnet near  $T_C$ .<sup>5</sup> This is true for La-Ca manganites as well.<sup>33</sup> In this case, according to Refs. 39 and 40, the longitudinal sound velocity should show a dip near  $T_C$  independent of the direction of propagation for both the isotropic and anisotropic materials. A situation with the transversal waves is more delicate. It is predicted in general<sup>39,40</sup> that the transverse ultrasonic anomaly should be less in magnitude than that for the longitudinal waves. Besides, the transverse-wave effect is significantly anisotropic being very small for some directions. In polycrystalline samples therefore no large transverse effect can be expected. Maybe for this reason the temperature behavior of the transverse sound does not reveal some distinct anomaly near  $T_C$  in contrast to the longitudinal waves (Figs. 6 and 7).

For an isotropic solid-state medium (as the polycrystalline sample studied with the pseudocubic perovskite lattice can be considered in the first approximation) the following expressions for the longitudinal and transverse sound velocities are known:

$$s_L(T, H) = \sqrt{\frac{E(1 - \sigma)}{d(1 + \sigma)(1 - 2\sigma)}} = \sqrt{\frac{K + 4G/3}{d}}, \quad (1)$$

and

$$s_T(T, H) = \sqrt{\frac{E}{2d(1 + \sigma)}} = \sqrt{\frac{G}{d}}, \quad (2)$$

where  $E$  is the Young's modulus,  $\sigma$  is the Poisson's ratio,  $K$  is the bulk modulus,  $G$  is the shear modulus,  $d$  is the mass density. The magnitudes of the moduli  $E$ ,  $G$ ,  $K$ , and that of the ratio  $\sigma$  are connected by the relations

$$G = \frac{E}{2(1 + \sigma)}, \quad K = \frac{E}{3(1 - 2\sigma)}, \quad (3)$$

so that, actually, the velocity  $s_L$  is determined by two independent moduli only, whereas  $s_T$  depends on the shear modulus  $G$  alone. The reciprocal of the bulk modulus  $K$  is the compressibility. It is clear that great softening of the longitudinal velocity near  $T_C$  found in this study (Figs. 3 and 8) is



connected with a decrease in the moduli's magnitude (or increase in the compressibility, which usually peaks at the PM-FM transition).

Consider more closely the effect of magnetic field on the longitudinal sound propagation. It is seen that the  $s_L(T)$  anomaly widens in magnetic field and its temperature position ( $T_{ir}$ ) moves to higher temperature with increasing field (Figs. 8 and 9). With decreasing temperature from above  $T_C$  the longitudinal velocity  $s_L$  softens due to developing the inhomogeneous magnetic state when moving closely enough to  $T_C$ . After crossing  $T_C$ , the velocity  $s_L$  starts to increase as the system becomes more homogeneous after transition to the FM state and arrives at far more magnitude than that above  $T_C$  (Fig. 3). It is evident that the temperature  $T_{ir}$  indicates, actually, the point of the most inhomogeneous state, and this temperature can be taken as the temperature of the PM-FM transition in the zero and nonzero magnetic fields. It is quite expected that the temperature of the first-order PM-FM transition is shifted under the influence of magnetic field. This is well known for La-Ca manganites as well. For example,  $T_C$  of  $\text{La}_{1-x}\text{Ca}_x\text{MnO}_3$  ( $x=0.33$ ) with  $T_C \approx 260$  K in zero field moves to higher values in magnetic fields with the rate  $dT_C/dH=19$  K/T.<sup>44</sup> For the sample studied this quantity (taken on cooling) is about 10 K/T (as can be easily estimated from Fig. 9). This is somewhat less than that obtained in Ref. 44, but for the sample with smaller values of Ca concentration ( $x \approx 0.25$ ) and  $T_C$  ( $\approx 200$  K) this fairly comes up to expectations. It should be pointed out that the temperature position of the sharp resistance drop, corresponding to the PM-FM transition, moves to higher temperature as well with an increase in magnetic field (Fig. 2), so that, in this study, the resistive and magnetoresistive data agree fairly well with the ultrasonic ones.

Due to considerable hysteresis (Fig. 6), the values of  $T_{ir}(H)$  taken from the  $s_L(T)$  curves on heating,  $T_{ir}^{up}$ , and cooling,  $T_{ir}^{dn}$ , are essentially different, as expected for first-order transition. The difference ( $\Delta T_{ir}=T_{ir}^{up}-T_{ir}^{dn}$ ) reduces, however, nearly to zero with increasing magnetic field up to  $H=4$  T (Fig. 9). It appears that the transition changes from first to second order under the influence of external magnetic field. The case when a first-order transition becomes second, as an external parameter is varied, is considered in Ref. 46. This theory takes into account that the coherence length  $\xi$  remains finite at a first-order transition. If this length is sufficiently large near the phase transition to "average out" the existing (intrinsic and extrinsic) inhomogeneities, the transition is sharp, as it should be for a first-order transition. If, on the other hand, the growth of correlations with moving to the transitions is blocked by inhomogeneities of a different kind, the transition becomes "smeared out" and looks like a second order (the same effect can be induced by extrinsic inhomogeneities<sup>4</sup>). The application of magnetic field can increase the degree of magnetic inhomogeneity in manganites (enhancing the mixed-phase state near the transition point) for different reasons<sup>4</sup> and leads therefore to significant rounding of a transition, so that at a sufficiently high field a first-order transition appears as (or becomes) second order. It is really seen in Fig. 8 that the  $s_L$  anomaly becomes broader and more smeared with increasing field, that corresponds to the pattern outlined in Ref. 46.

The magnetic behavior of  $\Delta T_{ir}=T_{ir}^{up}-T_{ir}^{dn}$  found in this study corresponds in general to the main conception of Ref. 47 for disorder-broadened first-order transitions. The authors of that work suppose generally that  $\Delta T_{ir}$  (which they called the temperature window of transition) must decrease (increase) with increasing some influencing parameter for transitions in which  $T_C$  rises (falls) with that parameter. This statement is true for our case if the magnetic field is taken as the influencing parameter. It is interesting to note that this rule is also true for the manganites (for example,  $\text{Nd}_{1/2}\text{Sr}_{1/2}\text{MnO}_3$  and others<sup>48</sup>) which undergo the transition from the FM to antiferromagnetic (or charge-ordered) state with decreasing temperature. In this case the application of magnetic field causes a decrease in  $T_N$  (or  $T_{CO}$ ) which is accompanied by an increase in  $\Delta T_{ir}$ . This effect in  $\text{Nd}_{1/2}\text{Sr}_{1/2}\text{MnO}_3$  for the charge-ordering transition has found its confirmation in ultrasonic study<sup>49</sup> as well.

Figure 10 demonstrates that the longitudinal sound velocity  $s_L$  is fairly sensitive to changes in magnetic state of the manganites induced by magnetic field. As indicated above, a strengthening of FM order (and corresponding decrease in the specific volume) leads to an increase in  $s_L$ . The ability of an external magnetic field to increase the magnetization can explain in general terms the behavior  $s_L(H)$  below  $T_C$  (Fig. 10). It is clear that at low temperature ( $T \ll T_C$ ) when nearly all spins are already aligned by the exchange interaction, this ability is minimal. For this reason, the longitudinal MSE is very weak for  $T \ll T_C$ , but is enhanced profoundly with increasing temperature remaining positive and monotone below  $T_C$ . The things get changed when temperature rises close enough to and above  $T_C$ . Here, on the one hand, the possibility to strengthen the magnetic order with an external magnetic field increases profoundly, since the magnetic order becomes weaker; on the other hand, however, the application of magnetic field increases inhomogeneity in manganites (enhancing the mixed-phase state near transition) and leads to significant rounding of the transition. The competition of these two mechanisms results in the minimum in  $s_L(H)$  in this temperature range (Fig. 10). With increasing field,  $s_L(H)$  at first decreases due to developing inhomogeneous magnetic state (inducing the negative MSE) and then, with further increasing field, it rises due to strengthening of the FM order (increase in the saturation magnetization in the paraproces).

The temperature behavior of the transverse velocity  $s_T(T)$  does not show any pronounced anomaly in the region of PM-FM transition (Fig. 7). The same is true for magnetic-field behavior  $s_T(H)$  near and above  $T_C$  (Fig. 11). Below  $T_C$  the behavior of  $s_T(H)$  is nonmonotonic with a minimum in the field region of the technical saturation of the magnetization. According to our data, this saturation takes place at  $H_s \approx 0.03$  T below 100 K. Above  $H_s$  (that is in the paraproces) the transverse MSE is positive (Fig. 11). The field  $H_s$  goes to zero with temperature rising to  $T_C$ , so that the minimum in  $s_T(H)$  disappears near  $T_C$ .

In conclusion, the peculiarities of the PM-FM transition in the sample of  $\text{La}_{1-x}\text{Ca}_x\text{MnO}_3$  ( $x=0.25$ ) prepared by the floating-zone method have been studied by transport, magnetic, and ultrasonic measurements. In particular, a sharp peak in the ultrasonic attenuation together with a very sharp

dip (softening) in the longitudinal sound velocity  $s_L$  have been found near the Curie temperature. This is in contrast with previous ultrasonic studies of manganites of the approximate composition where mainly only a pronounced increase in  $s_L$  (Refs. 1, 24, and 25) or a very slight dip<sup>26,27</sup> as a result of the PM-FM transition was found. We attribute this to a rather disordered polycrystalline state of the samples studied in those references that resulted in smearing out the magnetic transition. Our results indicate that the PM-FM transition in the sample studied is first order. This transition, however, can become second order under the influence of the

high enough applied magnetic field which increases a degree of inhomogeneity in the region near  $T_C$ . This behavior corresponds in general to the known theoretical model.<sup>46</sup>

## ACKNOWLEDGMENTS

We wish to thank V. D. Fil and A. A. Zvyagin for helpful suggestions and V. M. Stepanenko (Institute for Single Crystals, National Academy of Sciences, Kharkov, Ukraine) for compositional analysis of the sample studied.

\*Electronic address: belevtsev@ilt.kharkov.ua

<sup>1</sup>A. P. Ramirez, *J. Phys.: Condens. Matter* **9**, 8171 (1997).

<sup>2</sup>J. M. D. Coey, M. Viret, and S. von Molnar, *Adv. Phys.* **48**, 167 (1999).

<sup>3</sup>K. H. Kim, M. Uehara, V. Kiryukhin, and S-W. Cheong, in *Colossal Magnetoresistive Manganites*, edited by T. Chatterji (Kluwer Academic, Dordrecht, The Netherlands, 2004).

<sup>4</sup>B. I. Belevtsev, *Fiz. Nizk. Temp.* **30**, 563 (2004) [*Low Temp. Phys.* **30**, 421 (2004)].

<sup>5</sup>K. P. Belov, *Magnetic Transitions* [in Russian] (Gosudarstvennoe. Izdatel'stvo Fiziko-Matematicheskoi Literaturi, Moscow, 1959).

<sup>6</sup>B. I. Belevtsev, D. G. Naugle, K. D. D. Rathnayaka, A. Parasiris, and J. Fink-Finowicki, *Physica B* **355**, 341 (2005).

<sup>7</sup>E. A. Masalitin, V. D. Fil, K. R. Zhekov, A. N. Zholobenko, T. V. Ignatova, and Sung-Ik Lee, *Low Temp. Phys.* **29**, 93 (2003) [*Low Temp. Phys.* **29**, 72 (2003)].

<sup>8</sup>D. Shulyatev, S. Karabashev, A. Arsenov, Ya. Mukovskii, and S. Zverkov, *J. Cryst. Growth* **237-239**, 810 (2002).

<sup>9</sup>R. Laiho, K. G. Lizunov, E. Lähderanta, P. Petrenko, V. N. Stamov, and V. S. Zakhvalinskii, *J. Magn. Magn. Mater.* **213**, 271 (2000).

<sup>10</sup>Bas B. Van Aken, A. Meetsma, Y. Tomioka, Y. Tokura, and Thomas T. M. Palstra, *Phys. Rev. B* **66**, 224414 (2002); B. B. Van Aken, Ph.D. thesis, University of Groningen, Groningen, The Netherlands, 2001, [www.ub.rug.nl/eldoc/dis/science](http://www.ub.rug.nl/eldoc/dis/science)

<sup>11</sup>F. Rivadulla, J. Rivas, and J. B. Goodenough, *Phys. Rev. B* **70**, 172410 (2004).

<sup>12</sup>Y. Lyanda-Geller, S. H. Chun, M. B. Salamon, P. M. Goldbart, P. D. Han, Y. Tomioka, A. Asamitsu, and Y. Tokura, *Phys. Rev. B* **63**, 184426 (2001).

<sup>13</sup>V. Markovich, Y. Yuzhelevskii, G. Gorodetsky, G. Jung, C. J. van der Beek, and Ya. M. Mukovskii, *Eur. Phys. J. B* **35**, 295 (2003).

<sup>14</sup>It follows from the known phase diagram of the  $\text{La}_{1-x}\text{Ca}_x\text{MnO}_3$  (Refs. 1–3) that  $T_C$  values should be about 250–260 K for  $0.3 \leq x \leq 0.35$  with lesser values (220–225 K) at  $x=0.25$ . This diagram was obtained, however, for ceramic samples prepared by the solid-state reaction method. In more perfect samples prepared by the floating-zone method,  $T_C$  values for  $0.22 \leq x \leq 0.35$  are usually smaller by 20–30 K (see discussion in Ref. 6).

<sup>15</sup>Y. B. Zhang, S. Li, P. Hing, C. Q. Sun, W. Cao, and S. X. Dou, *Solid State Commun.* **120**, 107 (2001).

<sup>16</sup>V. S. Amaral, J. P. Araújo, Yu. G. Pogorelov, P. B. Tavares, J. B.

Sousa, and J. M. Vieira, *J. Magn. Magn. Mater.* **242-245**, 655 (2002).

<sup>17</sup>M. B. Salamon and S. H. Chun, *Phys. Rev. B* **68**, 014411 (2003).

<sup>18</sup>We can point out for comparison some parameters for the sample in Ref. 6:  $\rho(T_p)/\rho(0) \approx 200$ , the activation energy in paramagnetic state  $E_a \approx 0.09$  eV, resistance minimum is at  $T_{min} \approx 16$  K, and maximum  $\Delta R(H)/R(0)$  are 84.4% and 93.1% at  $H=1$  and 2 T, respectively. It seems that the sample studied appears not less (or even more) perfect than that in Ref. 6.

<sup>19</sup>Y. Yuzhelevskii, V. Markovich, V. Dikovskiy, E. Rozenberg, G. Gorodetsky, G. Jung, D. A. Shulyatev, and Ya. M. Mukovskii, *Phys. Rev. B* **64**, 224428 (2001).

<sup>20</sup>T. R. McGuire and R. I. Potter, *IEEE Trans. Magn.* **MAG-11**, 1018 (1975).

<sup>21</sup>B. I. Belevtsev, V. B. Krasovitsky, D. G. Naugle, K. D. D. Rathnayaka, A. Parasiris, S. R. Surthi, R. K. Pandey, and M. A. Rom, *Phys. Status Solidi A* **188**, 1187 (2001).

<sup>22</sup>M. Ziese, *Phys. Rev. B* **62**, 1044 (2000).

<sup>23</sup>M. Ziese, *Rep. Prog. Phys.* **65**, 143 (2002).

<sup>24</sup>A. P. Ramirez, P. Schiffer, S-W. Cheong, C. H. Chen, W. Bao, T. T. M. Palstra, P. L. Gammel, D. J. Bishop, and B. Zegarski, *Phys. Rev. Lett.* **76**, 3188 (1996).

<sup>25</sup>Changfei Zhu and Renkui Zheng, *Phys. Rev. B* **59**, 11169 (1999); Changfei Zhu, Renkui Zheng, Jinrui Su, and Wenhai Shong, *J. Phys.: Condens. Matter* **12**, 823 (2000).

<sup>26</sup>Changfei Zhu, Renkui Zheng, Jinrui Su, and Jiang He, *Appl. Phys. Lett.* **74**, 3504 (1999).

<sup>27</sup>Hiroyuki Fujishiro, Tetsuo Fukase, Manabu Ikebe, and Tsutomu Kikuchi, *J. Phys. Soc. Jpn.* **68**, 1469 (1999).

<sup>28</sup>V. Rajendran, S. Muthu Kumaran, V. Sivasubramanian, T. Jayakumar, and Baldev Raj, *Phys. Status Solidi A* **195**, 350 (2003).

<sup>29</sup>Hiroyuki Fujishiro, Tetsuo Fukase, and Manabu Ikebe, *J. Phys. Soc. Jpn.* **70**, 628 (2001).

<sup>30</sup>J. Mira, J. Rivas, A. Moreno-Gobbi, M. Pérez Macho, G. Paolini, and F. Rivadulla, *Phys. Rev. B* **68**, 092404 (2003).

<sup>31</sup>P. G. Radaelli, D. E. Cox, M. Marezio, S-W. Cheong, P. E. Schiffer, and A. P. Ramirez, *Phys. Rev. Lett.* **75**, 4488 (1995).

<sup>32</sup>P. Dai, Jiandi Zhang, H. A. Mook, S.-H. Liou, P. A. Dowben, and E. W. Plummer, *Phys. Rev. B* **54**, R3694 (1996).

<sup>33</sup>M. R. Ibarra, P. A. Algarabel, C. Marquina, J. Blasco, and J. Garcia, *Phys. Rev. Lett.* **75**, 3541 (1995); J. M. de Teresa, M. R. Ibarra, P. A. Algarabel, C. Ritter, C. Marquina, J. Blasco, J. Garcia, A. del Moral, and Z. Arnold, *Nature (London)* **386**, 256 (1997).

- <sup>34</sup>Q. Huang, A. Santoro, J. W. Lynn, R. W. Erwin, J. A. Borchers, J. L. Peng, K. Ghosh, and R. L. Greene, *Phys. Rev. B* **58**, 2684 (1998).
- <sup>35</sup>S. J. Hibble, S. P. Cooper, A. C. Hannon, I. D. Fawcett, and M. Greenblatt, *J. Phys.: Condens. Matter* **11**, 9221 (1999).
- <sup>36</sup>P. G. Radaelli, G. Iannone, M. Marezio, H. Y. Hwang, S-W. Cheong, J. D. Jorgensen, and D. N. Argyriou, *Phys. Rev. B* **56**, 8265 (1997).
- <sup>37</sup>S. J. L. Billinge, Th. Proffen, V. Petkov, J. L. Sarrao, and S. Kycia, *Phys. Rev. B* **62**, 1203 (2000).
- <sup>38</sup>Jian-Min Li, C. H. A. Huan, You-Wei Du, Duan Feng, and Z. X. Shen, *Phys. Rev. B* **63**, 024416 (2000).
- <sup>39</sup>H. S. Bennet and E. Pytte, *Phys. Rev.* **155**, 553 (1967).
- <sup>40</sup>B. Lüthi, T. J. Moran, and R. J. Pollina, *J. Phys. Chem. Solids* **31**, 1741 (1970).
- <sup>41</sup>M. Tachiki and S. Maekawa, *Prog. Theor. Phys.* **51**, 1 (1974).
- <sup>42</sup>G. Papavassiliou, M. Fardis, M. Belesi, T. G. Maris, G. Kallias, M. Pissas, D. Niarchos, C. Dimitropoulos, and J. Dolinsek, *Phys. Rev. Lett.* **84**, 761 (2000).
- <sup>43</sup>M. García-Hernández, A. Møllergård, F. J. Mompeán, D. Sánchez, A. de Andrés, R. L. McGreevy, and J. L. Martínez, *Phys. Rev. B* **68**, 094411 (2003).
- <sup>44</sup>D. Kim, B. Revaz, B. L. Zink, F. Hellman, J. J. Rhyne, and J. F. Mitchell, *Phys. Rev. Lett.* **89**, 227202 (2002).
- <sup>45</sup>C. P. Adams, J. W. Lynn, V. N. Smolyaninova, A. Biswas, R. L. Greene, W. Ratcliff, II, S-W. Cheong, Y. M. Mukovskii, and D. A. Shulyatev, *Phys. Rev. B* **70**, 134414 (2004).
- <sup>46</sup>Y. Imry and M. Wortis, *Phys. Rev. B* **19**, 3580 (1979).
- <sup>47</sup>S. B. Roy and P. Chaddah, *Curr. Sci.* **88**, 71 (2005); P. Chaddah, cond-mat/0602128 (unpublished).
- <sup>48</sup>Y. Tomioka, A. Asamitsu, H. Kuwahara, and Y. Tokura, in *Physics of Manganites*, edited by T. A. Kaplan and S. D. Mahanti (Kluwer/Plenum, New York, 1999), pp. 155–175.
- <sup>49</sup>S. Zvyagin, H. Schwenk, B. Lüthi, K. V. Kamenev, G. Balakrishnan, D. McK. Paul, V. I. Kamenev, and Yu. G. Pashkevich, *Phys. Rev. B* **62**, R6104 (2000).